J. Membrane Biol. 100, 31–42 (1987)

The Journal of
Membrane Biology

Steady-State Voltage-Dependent Gating and Conduction Kinetics of Single K^+ Channels in the Membrane of Cytoplasmic Drops of *Chara australis*

D.R. Laver and N.A. Walker
Biophysics Laboratory, School of Biological Sciences, University of Sydney A12, New South Wales 2006, Australia

Summary. Cytoplasmic drops, covered by a membrane derived from the tonoplast, were obtained from the internodal cells of *Chara australis*. Patch-clamp measurements were made on this membrane using the droplet-attached configuration with the membrane patch voltage clamped at values from −250 to 50 mV. Single-channel records, filtered at 5 kHz, were analyzed to elucidate the kinetics of the ion gating reaction of the K^+-selective channel. The current-voltage characteristics for single channels exhibit saturation and are shown to be consistent with Läuger's theory of diffusion-limited ion flow through pores (P. Läuger, *Biochim. Biophys. Acta* **455**:493–509, 1976). The time-averaged behavior of the K^+ conductance has a maximum at −100 to −150 mV which is produced by the combination of two distinct mechanisms: (1) The channel spending more time in long-lived closed states at positive voltages and (2) a large decrease in the mean open lifetime at more negative voltages. The channel activity shows bursting behavior with opening and closing rates that are voltage-dependent. The mean open time is the kinetic parameter most sensitive to membrane potential, showing a maximum between −100 to −150 mV. The distribution of open times is dominated by one exponential component (time constant 0.3 to 10 msec). In some cases an additional rapidly decaying exponential component was detectable (time constant = 0.1 msec). The closed distributions contained were observed to obtain up to four exponential components with time constants over the range 0.1 to 200 msec. However, the voltage dependence of the closed-time distributions suggests an eight-state model for this channel.

Key Words patch clamp · K^+-channels · cytoplasmic drops · gating kinetics · voltage dependence · *Chara australis*

Introduction

Cytoplasmic drops, retaining many of the properties of intact cells, can be isolated from the internodal cells of charophytes (Kamiya & Kuroda, 1957). Cytoplasmic drops consist of a drop of cytoplasm delineated by a membrane which exhibits excitability (Inoue, Ishida & Kobatake, 1973), ion selectivity (Inoue et al., 1973; Reeves, Shimmen & Tazawa, 1985) and light-induced active transport (Svintitskikh, Andrianov & Bulychev, 1985). Recent experiments in which the vacuolar compartment of charophyte cells were perfused with a fluorescent label identified the droplet membrane as being derived largely from the tonoplast (Lühring, 1986; Sakano & Tazawa, 1986). A recent patch-clamp study on membranes of cytoplasmic drops isolated from *Chara australis* (Lühring, 1986) reported that the most frequently observed ion translocator in the membrane surrounding these drops is highly selective for K^+ (P_K/P_{Na} and P_K/P_{Cl} greater than 100). He showed that the unitary current-voltage relation for this channel exhibited saturating behavior such as expected for an ion-translocating mechanism whose current is limited by diffusion in the medium outside the channel. He also noted that the rates of occurrence of the opening and closing transitions were dependent on the transmembrane electric potential difference (membrane potential) and that the channel activity shows bursting behavior typical of most other ion channels.

Cytoplasmic drops are a particularly convenient model for patch-clamp studies on the membrane of *Characean* cells as they can be prepared quickly and easily. The membrane delineating these cytoplasmic drops is directly accessible to the patch pipette and readily forms stable, high-resistance seals with the pipette tip. In this work the patch-clamp technique is applied to cytoplasmic drops isolated from internodal cells of *Chara australis* to study the steady-state electrical and kinetic properties of K^+ channels. Further, we examine the time-averaged steady-state electrical behavior of the K^+ channel and how it is related to single-channel events.

A quantitative analysis of the unitary current-voltage (I/V) relation of the K^+ channel is presented in terms of Läuger's theory of diffusion-limited ion flow through pores (Läuger, 1976). The voltage-dependent kinetics of the opening and closing transitions of the K^+ channel are examined in detail. The frequency distributions of the open and closed dura-

tions at different membrane potentials are presented and a kinetic model which is consistent with this channel activity is proposed. The voltage-dependence of the K^+ current through many channels in a single patch as well as the time-averaged currents through single channels are compared with that found for K^+ channels in other membrane systems determined from patch-clamp and whole-cell voltage-clamp studies.

Conceptual Framework

The theory for dealing with the kinetics of ion channels has been described by Colquhoun and Hawkes (1981, 1982, 1983). Some of the concepts fundamental to the analysis of channel kinetics are summarized here. Consider a hypothetical ion-gating reaction described by the kinetic model shown here.

Scheme 1:

$$\begin{array}{lccccc} & C & \underset{q_{12}}{\overset{q_{21}}{\rightleftharpoons}} & C & \underset{q_{23}}{\overset{q_{32}}{\rightleftharpoons}} & O \\ \text{state \# } & 1 & & 2 & & 3 \end{array}$$

where q_{ij} are the reaction rate constants for the transitions between states. The probability $f(t)$ that the channel having entered any particular group of states A, at $t = 0$ will exit from that group in the time interval t to Δt is called the probability distribution function of the channel lifetime in A. This function is given by:

$$f(t) = \lim_{\Delta t \to 0}[\text{Prob(Duration in } A \text{ is between } t \text{ and } t + \Delta t)/\Delta t]. \tag{1}$$

It can be shown (Colquhoun & Hawkes, 1981) that the time spent in a group of m kinetically distinct states has the form

$$f(t) = \sum_{n=1}^{m} P_n \cdot \exp[-Q_n \cdot t] \tag{2}$$

where P_n and Q_n depend on the rate constants and the kinetic model. For example the probability distribution function of the closed times (states 1 and 2 in A) of channel current fluctuations described by the above model will be the sum of two exponentials. The probability distribution function of open- and closed-times have the same form as the open- and closed-time frequency distributions.

Ion gating kinetics modelled by an open state connected with several closed states with very different mean lifetimes will exhibit bursting behavior, i.e. clustering of rapid activity into bursts which are separated by relatively long dormant periods. The kinetic reactions responsible for a burst in the above model (when q_{23} is much greater than q_{12}) would be a series of transitions between states 2 and 3 followed by a period in state 1. A channel with three distinct closed states will also manifest clusters of bursts within the patch-clamp record. In general the time spent within bursts and burst clusters represents sojourns in a group of states A containing at least one open state and one closed state.

Materials and Methods

Cytoplasmic drops are formed by the effusion of cytoplasm from the internodal cells of *Chara australis* R. Brown (Kamiya & Kuroda, 1957) into an aqueous medium which is isotonic with the vacuolar sap. The cytoplasmic drops were prepared by the same method as that used by Lühring (1986). The composition of the bathing medium was usually 144 mM KCl, 5 mM $CaCl_2$, 5 mM H^+MES and adjusted to a pH of 5.1 to 5.6 using KOH. All solutions were filtered with a 0.22-μm filter (Millipore) before use. The temperature of the bathing medium was monitored using a calibrated thermistor which was kept electrically isolated from the bath. The bath solution was maintained at ground potential by immersing an Ag/AgCl electrode connected to earth via the head stage of the patch-clamp amplifier (LIST EPC7).

Patch pipette electrodes were pulled from borosilicate glass microcapillary tubes (Hilgenberg, Mansfeld) with an internally fused element to facilitate easy filling. The desired pipette tape and tip diameter was achieved with a two-stage pull on a vertical electrode puller (David Kopf model 720) using a platinum ribbon heating element. Fire polishing and Silgard® coating of the electrodes was not necessary for obtaining good patch-clamp records so these procedures were omitted. The composition of the electrode filling solution was always kept the same as that of the bathing solution. The patch pipette was held in a pressure-tight assembly which in turn was carried on a hydraulic micromanipulator (Narishige model M0-8).

During experiments the output of the patch-clamp amplifier was simultaneously displayed on a CRO and recorded on magnetic tape (TDK SAX-90 cassettes) with an FM data recorder (TEAC model R-80) using a low-pass four-pole bessel filter set at 5.5 kHz (−3 dB) incorporating phase compensation to eliminate ringing. A computer (IBM-AT) interfaced to the experiment with a multipurpose I/O device (DT2801-A) was used to digitize and analyze the patch-clamp recordings. Calibration of the overall gain of the FM data recorder and computer interface were made at the beginning and end of each tape cassette using a known square-wave voltage signal. Continuous data sampling, storage on hard disc and subsequent graphical display of the digitized data was effected using the programs ADCIN and SCOPE (from Dr. J. Pumplin, Dept. of Physics, Michigan State University). The software package (IPROC2 from Dr. C. Lingle, Dept. of Biological Sciences, Florida State University) used for the detection and analysis of single-channel current fluctuations, is an adaption of software written by F. Sachs and J. Neil. Sachs (1983) discusses the principles of the automated analyses that are used here. Patch-clamp measurements were performed with the pipette and cytoplasmic drop in the drop-attached configuration (Hamill et al., 1981). Electrode voltages were compensated before the membrane-pipette seal was formed. Measuring the tip resistance of the electrode and monitoring the formation of the membrane-pipette seal was facilitated by applying a square-wave voltage signal (1-mV amplitude) superimposed on the voltage-clamp command potential. Once seal formation had occurred the pipette potential was clamped to a random sequence of values, at 100- to 200-sec intervals, over the range −100 to 300 mV. The membrane resting potential was measured at the end of each experiment by breaking the membrane patch, thus providing electrical contact between the patch electrode and the drop interior. Provided the membrane resting potential does not vary significantly during the course of the experiment then the electric potential difference across the membrane patch V_m can be calculated from the following equation:

$$V_m = V_r - V_{pip}$$

where V_r is the measured membrane resting potential and V_{pip} is the voltage-clamp potential of the pipette electrode. The open-time frequency distributions were fitted with exponential functions using the nonlinear least-squares fitting routine, NFITS, incorporating subroutines from the IMSL statistics library.

The kinetic analysis program, IPROC2, divides the records of channel activity into bursts. These are phenomenologically defined as periods of current fluctuations terminated by closed periods exceeding a predetermined threshold. Thus all closed periods within bursts, so defined, are shorter than this threshold value. The burst is the basic unit of channel activity scrutinized by IPROC2 during the analysis procedures. Bursts showing double-current steps were automatically rejected to ensure that only single-channel kinetics were examined. In general the kinetic parameters were derived from membrane patches where only one channel was evident, using criteria for assuming that the channel activity is derived from only a single channel as described by Colquhoun and Hawkes (1981). However, kinetic parameters, derived from records where limited dual-channel activity was evident (less than 10% of bursts having double-current steps), were still considered as valid descriptions of single-channel characteristics. Analysis of the current records usually involved two passes of the data each using different criteria for scrutinizing bursts of activity. This was done to check for artifacts arising from bias in the automated detection of valid single-channel events.

The probability distribution functions of the open and closed times and bursting behavior predicted by theoretical kinetic models were calculated numerically using the Q-matrix method of Colquhoun and Hawkes (1981, 1982). The theoretical predictions allow for the effects of brief missed events in the current records using the effective rate constant method of Blatz and Magleby (1986).

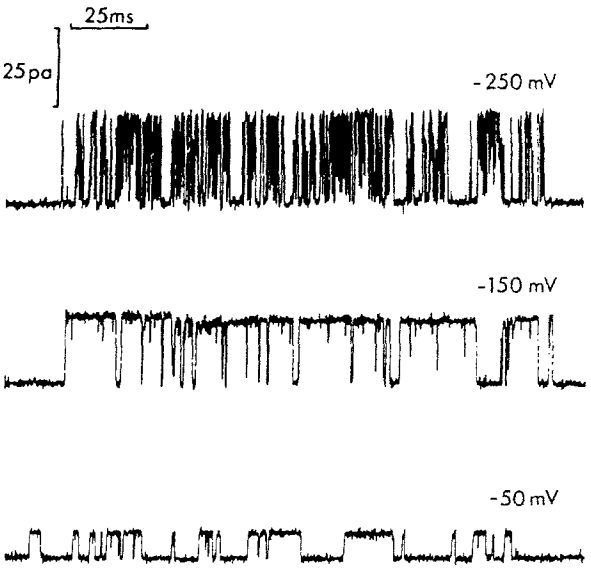

Fig. 1. Shown here are records of current fluctuations (as appearing at the output of the patch-clamp amplifier) typical of bursts of potassium channel activity at three different values of the membrane potential V_m. The current baseline is toward the bottom of each trace. The current convention in this Figure is positive current passing out of the patch pipette, i.e. negative membrane currents when using the membrane-attached configuration. The frequency resolution shown here is 5 kHz. The small downward current spikes on the upper parts of each trace are partly resolved, very short closures of the K^+ channel. The most striking difference between these records is the relatively large number of rapid fluctuations introduced at −250 mV

Results

General Observations

Cytoplasmic drop samples were found to contain a wide variety of droplet sizes. In this study patch-clamp measurements were made on droplets with diameters larger than 10 μm. The appearance of the cytoplasmic drops was similar to that described by Lühring (1986). The electrode resistances in the bathing solutions were typically 10 to 20 MΩ. High-resistance seals (10 to 50 GΩ) between the pipette and droplet were stable and formed readily. Within an hour of preparation the ability of the droplet membranes to seal against the pipette had deteriorated to the point where further measurements were not feasible. Seal resistances were markedly more stable at positive pipette potentials (i.e. negative membrane potentials in the drop attached configuration) than at negative potentials. Seal breakdown at negative pipette potentials made it difficult to obtain records of sufficient length for kinetic analysis. The membrane resting potentials of nine cytoplasmic drops were observed to be in the range −10 to +10 mV. The combined background random current noise of the apparatus and the pipette-drop system was less than 1 pA (rms) with a band width of 5 kHz.

K^+ channels were found to be the most frequently detected channel in these experiments. These channels could be easily identified by their unusually large currents which have been well characterized by Lühring (1986). Record lengths of about 100 sec are sufficient for kinetic analysis as the K^+ channels are very active. The appearance of the current records varies considerably with membrane voltage (*see* Fig. 1). At small membrane potentials (−50 to +50 mV) they consist of short pulses separated by relatively long closed periods. As the membrane potential is hyperpolarized beyond −75 mV the closed periods become shorter and bursting behavior is apparent. Very short, partly resolved closings of the channel can be detected at these voltages. At larger voltages (more negative than −200 mV) the current pulses become

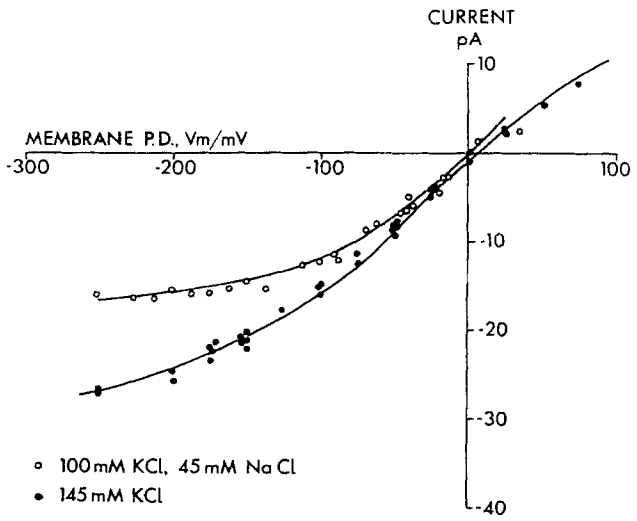

Fig. 2. Unitary current-voltage characteristics of the K^+-selective channel. The data shown here are the combined results of five experiments using electrode-filling solutions with pH 5.1 to 5.6 and containing 144 mM KCl, 5 mM $CaCl_2$, 5 mM MES at 21°C (●) and four experiments with solutions containing 100 mM KCl, 45 mM NaCl, 5 mM $CaCl_2$, 5 mM MES at pH 5.1 and 28°C (○). The membrane potential V_m is measured with respect to the exterior bath solution. The convention of outward current being given positive sign is adopted here. The solid curves show the numerical solutions to the simultaneous Eqs. (3)–(5). The parameter values used in the equations are listed in Table 2

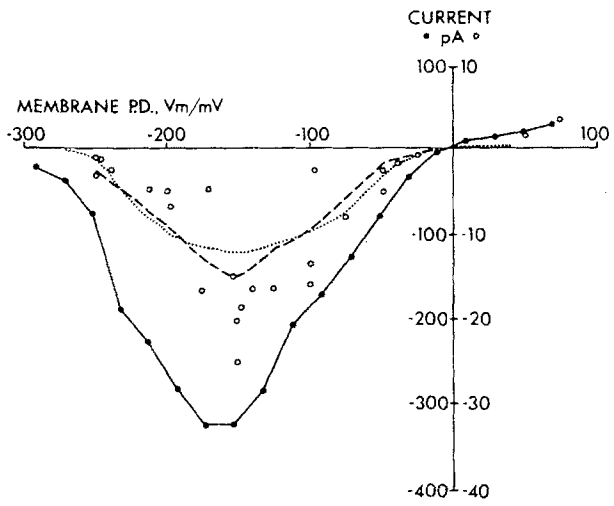

Fig. 3. Time-averaged I/V relation for: (○) single K^+ channels at 21°C in 144 mM KCl, 5 mM $CaCl_2$ and 5 mM MES with pH 5.1 to 5.6; (●) a patch containing an estimated 20 individual K^+ channels in a solution of 100 mM KCl, 45 mM NaCl, 5 mM $CaCl_2$ and 5 mM MES with pH 5.1 at 28°C. The potential difference V_m is defined with respect to the external solution and negative current is defined as positive charge flowing into the cytoplasmic drop. The dotted line indicates the predictions of the kinetic model (scheme 3). The dashed curve shows the I/V relation reconstituted from the data shown in Figs. 4 and 5

very short and the bursts are separated by long closed periods. Occasionally the number of electrically active channels in a patch would change indicating the existence of 'sleeping' channels.

Current-Voltage Curves

The unitary current-voltage (I/V) characteristics of open K^+ channels are shown in Fig. 2. The measured accuracy of the clamp current was ±2% or ±0.2 pA. Variations in I/V characteristics recorded from different patches were less than ±5% or ±1 pA. The I/V relation shows saturating behavior at large values of V_m and the magnitude of the saturation current is dependent on the K^+ concentration in the bathing medium. Figure 3 compares the voltage-dependent behavior of the single-channel time-averaged K^+ channel current from six membrane patches with that for a patch containing approximately 20 channels. It is apparent from Fig. 3 firstly, that the time-averaged behavior of individual channels is similar to that of many channels in a patch and secondly, that ion translocation through K^+-selective channels is largely restricted to the voltage range −250 to 0 mV with a maximum current at about −150 mV.

Single-Channel Kinetics

The frequency distributions of the closed-times in most cases could be adequately fitted with a function comprising the sum of three exponentials with time constants ranging from 0.1 to 100 msec. Four exponential components were required to fit the closed-time distributions when the membrane potentials were near −250 mV.

Figure 4 shows the frequency distributions of closed-times derived from a single membrane patch which was clamped at seven different voltages over the range −50 to −250 mV and also from a patch voltage clamped at 50 mV. It can be seen from Fig. 4 that the shapes of the closed-time distributions are affected by the membrane potential.

The frequency distributions of the channel open times are shown in Fig. 5 fitted with single exponentials. A small additional exponential component (0.1-msec time constant) was sometimes evident which comprised 5 to 10% of the area under the open-time distribution. During analysis of the channel kinetics the burst termination closed-time threshold was set at different values for each pass of the current records. A relatively small threshold value of 0.6 to 1 msec was used in determining burst durations and a longer threshold value of 6 to 10 msec where chosen to terminate clusters of burst

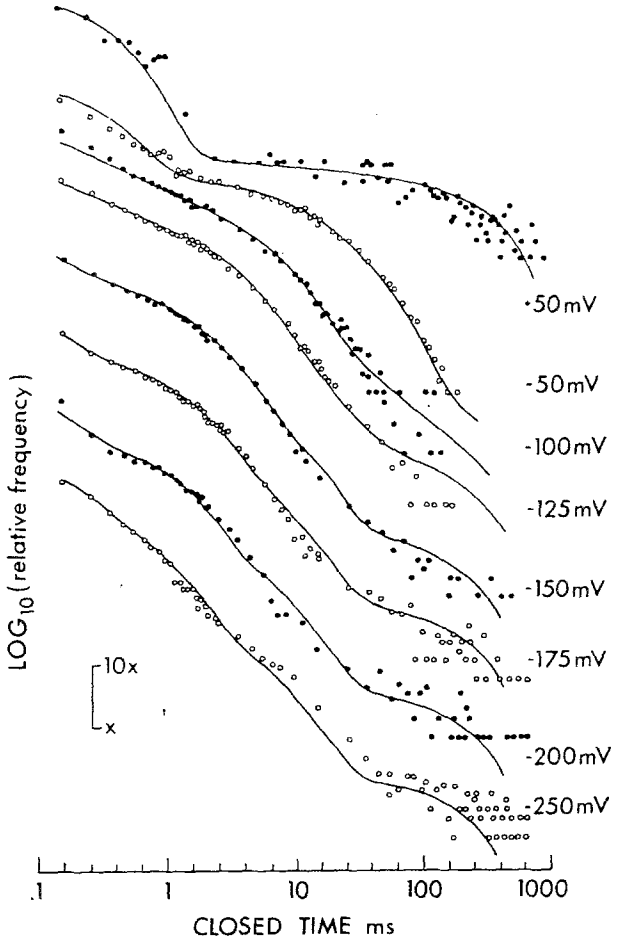

Fig. 4. Frequency distribution of the closed times are shown plotted on a log-log scale. Variable bin sizes are used with widths ranging from 0.1 to 10 msec. The data at each voltage have been displaced vertically for clarity. The full curves show the prediction of the kinetic model in reaction scheme 3

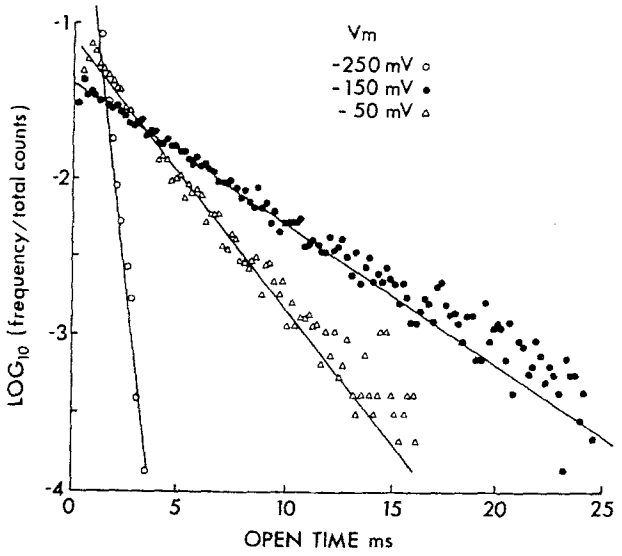

Fig. 5. Frequency distribution of channel open times is shown plotted on a log-linear scale. The binwidths are the same as in Fig. 4. The data here are shown fitted with single exponentials of the form $N \cdot \exp[-t/\tau]$

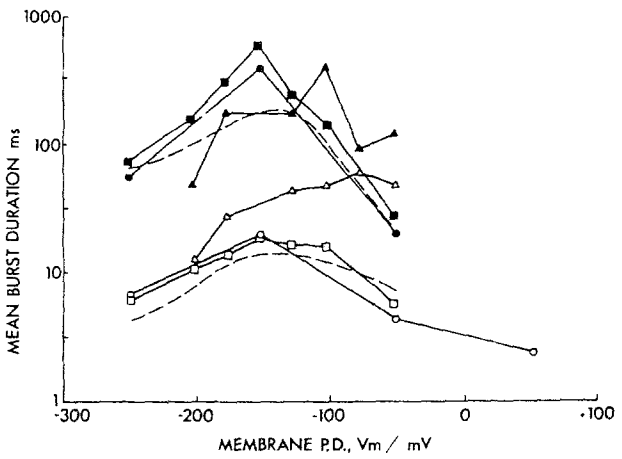

Fig. 6. Voltage-dependence of burst duration measured from three representative K⁻ channels. The closed symbols represent burst clusters separated by closed periods exceeding 10 msec. The open symbols depict bursts of activity within these clusters separated by closed periods exceeding 1 msec. The durations of bursts and burst clusters show a broad maximum at about −100 to −200 mV. The data shown as (□) and (■) are compared to the predictions of the kinetic model (scheme 3)

activity. Some of the burst duration values are shown in Fig. 6.

Figure 7 shows the mean fraction of time the K^+ channel spends in nonconducting states during each burst. The burst durations and fractional open times have strong voltage dependences which have broad maxima over the range −50 to −150 mV. When more than 80% of putative bursts within a current record were deemed as valid by IPROC2, the shapes of the closed- and open-time distributions were found to be insensitive to variations in the event detection- and analysis-criteria. Though considerable variation exists in the kinetic parameters calculated from K^+ channels situated in different membrane patches general trends in the voltage dependences were consistent. None of the kinetic properties of the K^+ channels showed any significant time dependence over periods of 10 min.

Discussion

Open-Channel *I/V* Characteristics

The conductance of the K^+ channel (in 150 mM KCl), derived from the maximum slope of the *I/V* data shown in Fig. 2, is 170 pS which is similar to

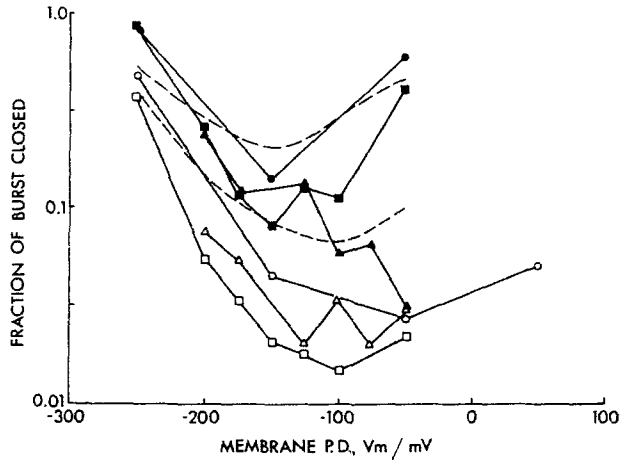

Fig. 7. Relative fraction of the burst durations spent in closed states. The data shown here is taken from the same records as that presented in Fig. 7. The symbols have the same meaning as in Fig. 7

Table 1. Summary of the analysis of the *I/V* data in Fig. 2 in terms of Läuger's (1976) theory of diffusion-limited ion flow through pores.

	100 mM KCl + 45 mM NaCl	145 mM KCl
P_c/P_i	2 (1.3 – 3)	2 (1.3 – 3)
$P_i \times 10^{19}$ m/sec	8.4 (6 – 11)	7.5 (6 – 10)
$P_c \times 10^{19}$ m³/sec	1.6 (1.4 – 1.8)	1.6 (1.4 – 1.8)
r_o nm	0.25	0.25
dI/dV_m (max) pS[a]	150	170
$\frac{P_i z^2 F^2}{RT}$ pS[b]	300 (230 – 400)	420 (330 – 550)

[a] The maximum conductance of the potassium channel and the adjacent electrolyte calculated from the slope of the *I/V* curves.
[b] The intrinsic conductance of the potassium-selective pore calculated from the predicted pore permeability.

that found for potassium channels in the membranes of other Charophyte cells (Ohkawa, Tsutsui & Kishimoto 1986). The current-voltage relationships for the open K^+ channel, shown in Fig. 2, are characteristic of diffusion-limited ion translocation across the pore. The solution of the Nernst-Planck equation has been calculated by Läuger (1976) for a single pore embedded in a membrane separating two aqueous phases as shown in Fig. 8. The theory considers a channel which is permeable to the cation species in an electrolyte also containing a non-permeable cation species and a common anion species. The net passive ion flux through such a channel has been calculated by solving numerically the simultaneous equations (Eq. 3–5):

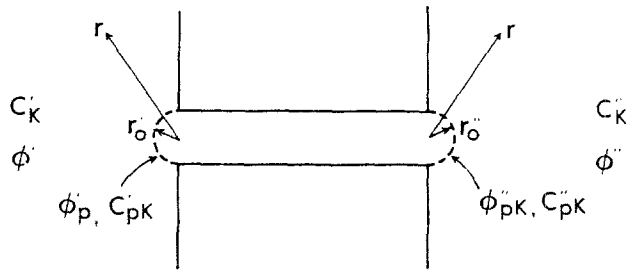

Fig. 8. From Läuger (1976). The geometric model of the pore upon which Eqs. (3)–(6) are based. The radial boundary between the interior and exterior of the pore is given by r_o, ϕ_p and C_{pk} are the reduced electrical potential and ion concentration of ion species k at the pore boundary. ϕ and C_k are the same quantities at infinite distance from the pore. The superscripts ' and " refer to the above quantities on the left- and right-hand-side, respectively

$$J = -2P'_cC_2 \cdot (y' - 1) \tag{3}$$

$$J = 2P''_cC''_2 \cdot (y'' - 1) \tag{4}$$

$$J = P_i \cdot [u + \ln(y'/y'')] \cdot \frac{\{U \cdot (C'_2y' - C'_3/y') - U^{-1}(C''_2y'' - C''_3/y'')}{U + U^{-1}} \tag{5}$$

where $y' \equiv \exp(\phi'_p - \phi')$, $y'' \equiv \exp(\phi''_p - \phi'')$ and $U \equiv [\exp(u) \cdot y'/y'']^{1/2}$, C_1 is the concentration of permeable cations, C_2 is the concentration of non-permeable cations, C_3 is the anion concentration, ϕ_p is the reduced electric potential near the mouth of the pore, ϕ is the reduced electric potential at infinity, P_i is the intrinsic permeability of the pore to ion species C_1, P_c is the permeability of the electrolyte near the mouth of the pore, u is the externally applied reduced electrostatic potential difference in units of F/RT, ' and " indicate parameters associated with the left and right sides of the pore, respectively.

P_c can be expressed in terms of the diffusion constant of the ion species in the aqueous phases.

$$P_c = 2\pi r_o D \tag{6}$$

where r_o is the effective ion capture radius of the channel which can be as small as the difference between the ion and pore radii.

The theoretical *I/V* relation was calculated for different values of P_i and P_c. The resulting curves which best fit the data are shown in Fig. 2. Table 1 contains the parameter value ranges over which the theoretical curves were consistent with the *I/V* data. The permeability of the external electrolyte is about two times larger than the intrinsic permeability of the pore. The slight difference between the values of P_c derived from the *I/V* relations in high

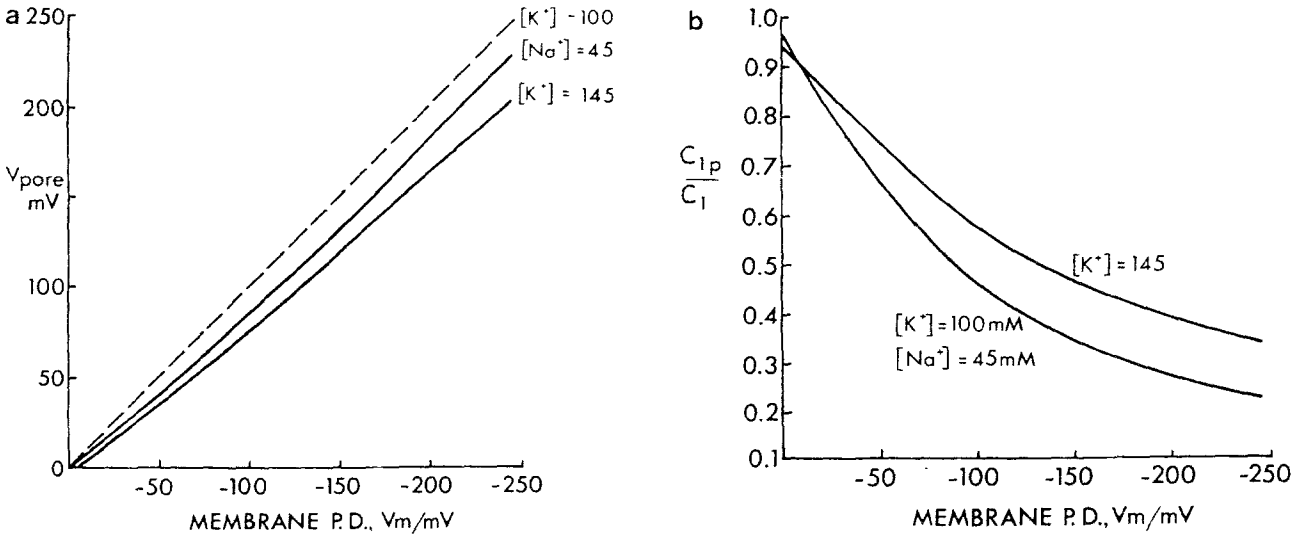

Fig. 9. (*a*) Transpore electrical potential difference $V_{pore} = (u + \ln y'/y'')$ as a function of membrane potential difference V_m calculated from Eqs. (3)–(6) using the parameter values listed in Table 1. The dashed line results when diffusion limitation effects are neglected. (*b*) Expected potassium concentration, C_{1p}, near the side of the pore which acts as the ion sink, relative to the bulk solution value under the same circumstances as in part (*a*)

and low K^+ concentrations is most likely due to the different temperatures at which the two sets of measurements were made. The capture radius of the pore, as calculated from Eq. (6) with $D = 10^{-9}$ is 0.25 nm. Therefore the radius of the pore can be up to 0.25 nm larger than that of the K^+ ion (i.e. pore radius is less than 0.4 nm).

The phenomenon of diffusion-limited ion flow has several consequences for the interpretation of intrinsic channel properties. Firstly, the intrinsic pore conductance is much larger than that derived from the slope of the *I/V* data (*see* Table 1). Secondly, the ion concentration and the electric potential near the mouth of the open channel will differ from that of the closed channel and from that detectable in the bulk solutions. Figures 9(*a*) and (*b*) show that in these experiments the trans-pore potential difference is as much as 50 mV lower than the membrane potential and the K^+ concentration at the pore mouth can be fourfold different from that found in the bulk phase. These effects should be considered when quantitatively predicting intrinsic properties of the K^+ channel.

Development of the Kinetic Model

The fact that at least three and sometimes four exponential terms were required to fit the closed-time distributions indicate that there are at least four distinct closed states involved in the ion gating reaction. The mean lifetimes of these closed states are spread over the range 0.1 to 200 msec. The open-time distributions indicate that one open state dominates the gating kinetics of this channel. The open-time distribution also indicates a short-lived open state (mean lifetime about 0.1 msec) which is detectable in some experiments. Due to the relative pausity of data concerning this short open state it can not, as yet, be reliably included in any kinetic model for ion gating. Consequently only the dominant, long-lived open state is considered in the putative kinetic scheme proposed here.

In any kinetic scheme the mean life of a state is equal to the inverse of the sum of the rate constants associated with reaction pathways leading away from that state. In the analysis of the kinetic model it is expected that the rate constants have an exponential dependence on membrane potential. If the K^+ could exit from its open state by only one route then the mean open-time would exhibit an exponential dependence on membrane potential like that which has been observed from some other channel types (Kolb, Köhler & Martinoia, 1987). The mean lifetime of the open state varies with voltage from 0.3 to 10 msec and has a maximum over the range −100 to −200 mV. Therefore there must be at least two reaction pathways connected to the open state (with opposite voltage dependences) to give a maximum in the voltage-dependence of the channel mean open time. The *minimum* kinetic scheme indicated so far is shown in

Table 2. Summary of the values of the rate constants associated with kinetic scheme 3 for K^+ channels from five membrane patches[a]

	Reaction rate constants from state x to y; $a[,b]$* sec^{-1}										
x,y	#1		#2		#3		#4		#5		uncertainty
A4,A3	10		10		25		25		35		±50%
A3,A4	40		40		100		100		100		±50%
A3,A2	250		250		250		250		250		±50%
A2,A3	240		340		140		200		200		±50%
A2,A1	2100		2100		2100		1700		2500		±20%
A1,A2	90000,	0.4	90000,	0.4	140000,	0.4	110000,	0.4	9000,	0.4	±50%,±20%
A1,0	8000		8000		8000		17000		5000		±20%
O,A1	3.6,	−0.7	2.5,	−0.8	1.9,	−0.74	6.0,	−0.6	10.0,	−0.6	±50%,±5%
O,B1	760,	0.25	2000,	0.4	430,	0.25	430,	0.25	250,	0.25	±10%,±20%
B1,O	2400		4000		3400		6000		4000		±20%
B1,B2	2000		2500		1000		1000		500		±20%
B2,B1	60,	−0.6	60,	−0.6	60,	−0.6	165,	−0.3	165,	−0.3	±30%,±10%
B2,B3	20		20		20		200		200		±50%
B3,B2	70		70		70		50		50		±50%

* Voltage-dependent rate constants are expressed in the form $a \cdot \exp(b \cdot eV/kT)$.

[a] The estimated uncertainty in the rate constants arising from fitting the predictions of the model to the kinetic data from each channel is shown in column 6.

Scheme 2:

$A \leftrightharpoons O \rightleftharpoons B$

where A and B are groups of one or more closed states, O is the open state, $q_{O-A} = (2\text{–}5) \cdot \exp(-(0.6\text{–}0.7)eV/kT)$ and $q_{O-B} = (250\text{–}2000) \cdot \exp((0.2\text{–}0.3)eV/kT)$.

A more detailed picture of the K^+ channel kinetics can be derived from the voltage dependence of the closed-time distribution data shown in Fig. 4. The ratio of q_{O-A}/q_{O-B} varies by five orders of magnitude from 70 at −250 mV to 7×10^{-4} at 50 mV. At positive voltages the channel kinetics is strongly biased to reactions involving the closed states B. Therefore the closed-time distribution data at more positive voltages mainly reflects the properties of the closed states in group B. Similarly at −250 mV the closed-time distribution should result primarily from the closed states in group A. Examining the closed-time distributions obtained at −250 mV and those at −50 and 50 mV it is found that group A is made up of four states and group B is comprised of three states. The interconnections between the closed states within groups A and B are not uniquely determined from the data. An example of a specific model that meets the above requirements is shown in scheme 3 in which the closed states within each group (A and B) are chosen to be connected in series with each other.

Scheme 3:

$A4 \rightleftharpoons A3 \rightleftharpoons A2 \rightleftharpoons A1 \rightleftharpoons O \rightleftharpoons B1 \rightleftharpoons B2 \rightleftharpoons B3.$

A wide variety of alternate kinetic models was compared with the data and in each case it was found that, provided the rate constants were constrained to follow exponential dependences on membrane potential, a minimum of seven closed states was required to fit the voltage dependence of the closed-time distributions. Kinetic scheme 3 represents the simplest model (i.e. with the minimum number of states, interconnections and voltage-dependent rate constants) which is consistant with the data in Figs. 3–7. Table 2 lists the rate constants associated with this model. Predictions of scheme 3, including the effects of the measured minimum event-duration detection limit of 50 μsec are compared with the data in Figs. 3–7. On the evidence presented here the kinetic model can at most be considered as a tentative proposition. However, this model will serve as a useful basis for further experiments.

Variability of Fitted Parameters

The I/V relations for open channels in membrane patches are found to have a relatively small variation compared with the variations in the parameters of their gating kinetics (*see* Table 2 and Fig. 10). The data-fitting procedures from which the kinetic parameters were derived, generated relatively little error. The automated analysis of patch-clamp records based on preprogrammed criteria for accepting or rejecting putative bursts is prone to bias the resulting frequency distributions. However, for

the results presented here the systematic errors arising from this bias were found to be small.

The main contribution to the scatter in the results seems to arise from variations intrinsic to the membrane patch. The variation in the fitted parameters of the gating kinetics is large, but the basic features of the channel kinetics are common to all the patches examined here. This observation indicates that the current fluctuations from different patches can be described by the same model but that there exist random factors probably external to the ion channel itself which are modulating the channel function. It is likely that these factors are associated with variations in the composition of the cytoplasm or the nature of the membrane environment near the channel.

Mean Channel *I/V* Relation

The multichannel *I/V* relation shows that a significant fraction of the K^+ channel population is open over the voltage range 0 to −250 mV. The time-average single and multichannel *I/V* characteristics are similar indicating that the electrical properties of the K^+ channel population can be accounted for in terms of the properties of isolated channels, i.e. the effects of cooperativity between channels can be neglected.

In order to understand the time-average behavior of the K^+ channel in terms of the observed K^+ channel kinetics the following procedure was adopted: the observed closed-time distributions of several channels were characterized by functions comprising the sum of three exponentials. In this way the data were characterized by a function with exponential time constants representing short-lived, medium and long-lived closed states. The relative time the channel spends in each of these states can then be calculated from the three exponential components of the fit. Together with the mean open times the time-averaged *I/V* relation for the channel could be reconstituted from the kinetic data. These procedures are summarized in Table 3. This approach has the advantage that it depends only on observable quantities and so its conclusions are model independent. A typical reconstituted mean *I/V* characteristic is compared with the data in Fig. 3. The similarity between the reconstituted values and the data (*cf.* columns 7 and 8 in Table 3) indicates that the properties of the observed *I/V* relation can be understood in terms of the kinetics of closed and open states in the range of durations 0.2 to 1000 msec. Hence the possible existence of long-lived closed states (mean lifetime > 1 sec) has little bearing on the single or multichannel mean *I/V* characteristics.

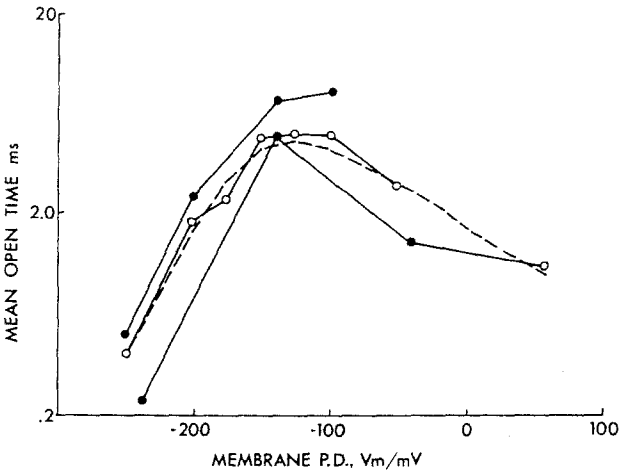

Fig. 10. Voltage dependence of the measured mean open durations for K^+ channels from different membrane patches plotted on a log-linear scale. The data depicted by (○) are compared with the predictions of the kinetic scheme 3 (dashed line)

Examining the relative contributions of the total times spent in the short, medium and long closed states and the open state reveals that the closure of channels at large and small membrane voltages arises from two distinct mechanisms: 1) a large increase in the time spent in long-lived closed states at positive voltages; 2) a large decrease in the mean open time of the channel at large negative voltages.

If the channels described here represent the tonoplast K^+ channels, then at their normal working voltage of −15 to −25 mV (Findlay & Hope, 1964; Spanswick & Williams, 1964; Spanswick, 1970) they would show a conductance intermediate between the highest value, at −150 mV, and the lowest, at positive voltages. This rectification may have physiological significance. If the combination of high K^+ concentrations and highly conductive K^+ channels is thought of as a mechanism for grabbing or clamping the membrane potential (Walker, 1980) then it will do so more efficiently for negative excursions of the tonoplast membrane potential (ϕ_{c-v}) than for positive ones. Such negative ones occur for example during the cell action potential, which involves a tonoplast action potential in which ϕ_{c-v} goes from −10 to −50 mV (Findlay & Hope, 1964).

This rectification will also have some effect on ion fluxes and concentrations: it will be easier for the movement of some ions to cause a flow of K^+ from vacuole to cytoplasm than from cytoplasm to vacuole. Flows in the former direction occur when, for example, the charophyte cell is exposed to amine, and the amine ions are accumulated in the vacuole in exchange for K^+ (Smith & Walker, 1978). The closing of K^+ channels at large negative

Table 3. Summary of the mean steady-state kinetic data for the potassium channel from four membrane patches[a]

	V_m (mV)	Closed-time (msec)				Open time (msec)	% open (Cal.)	% open (Exp.)
		#1	#2	#3	#4	#5	#6	#7	#8
#1	−50	22.0	0.04%	1.5%	98%	2.8	11%	21%
	−100	2.6	2.3%	35%	62%	4.8	64%	68%
	−125	2.2	2.7%	61%	36%	4.8	69%	72%
	−150	2.2	1.8%	58%	36%	4.9	70%	77%
	−175	2.9	1.0%	42%	55%	2.4	45%	57%
	−200	3.3	0.9%	30%	67%	1.9	36%	15%
	−250	4.4	3.2%	13%	91%	0.58	11%	9%
#2	−100	12.2	0.3%	4.6%	95%	8.0	40%	15%
	−150	2.8	1.1%	34%	64%	7.4	72%	77%
	−200	2.8	0.7%	29%	71%	2.6	48%	24%
	−250	4.9	1.4%	11%	86%	0.75	13%	4%
#3	−50	6.9	2.3%	5%	93%	7.9	53%	66%
	−100	3.6	2.5%	15%	83%	9.6	72%	24%
	−125	3.8	15%	23%	76%	11.0	72%	87%
	−175	2.4	0.8%	39%	62%	4.9	67%	51%
	−200	4.6	0.7%	19%	83%	2.4	34%	49%
#4	+50	61.9	0.05%	4.5%	95%	1.2	2%	0.6%
	−50	8.1	0.6%	18%	81%	1.5	16%	18%
	−150	2.0	2.5%	50%	56%	4.8	70%	77%
	−250	4.7	3.5%	15%	81%	0.42	8%	9%

[a] Columns 2 and 6 list the mean closed and open times, respectively. Columns 3, 4 and 5 contain the fraction of time spent in short, medium and long-lived closed states. Columns 7 and 8 compare the fraction of time the channel spends open calculated using different methods. Column 7 is calculated from the data in columns 2 and 6 and is used in conjunction with the unitary *I/V* characteristics to reconstitute the mean *I/V* relation shown in Fig. 3. Column 8 is experimentally derived from the ratio of the mean and unitary *I/V* data in Figs. 2 and 3.

potential differences is a feature of the channel activity which is common with K^+ channels in the plasmalemma of *Chara australis* (Beilby, 1986) but has no apparent purpose in the situation of the tonoplast.

There is a remarkable similarity between the voltage-dependence of the conductance of the population of K^+ channels in these droplets and that attributed to K^+ channels in the plasmalemma of *Chara* reported by Beilby (1985, 1986) and also by Coleman and Findlay (1985) with the plasmalemma in the K^+-sensitive state. Beilby (1985, 1986) measured the short-term (40 msec) current response of the plasmalemma to short voltage excursions from the membrane resting potential of *Chara australis* and Coleman and Findlay (1985) recorded the combined steady-state *I/V* characteristics of the plasmalemma and tonoplast of *Chara inflata*. In one respect this similarity with other K^+ channels in *Chara* is reassuring because it suggests that the properties of the K^+ channel studied here are not likely to have been altered during the cytoplasmic drop preparation procedures or significantly modified by the proximity of the patch pipette.

The K^+ conductance, determined from the maximum slope of the unitary *I–V* relation (170 pS) is similar to that found for the large conductance Ca^{2+}-activated K^+ channels in cultured rat muscle (230 pS) (Barrett, Magleby & Pallotta, 1982) and for Ca^{2+}-activated K^+ channels in acinar cells of the mouse lacrimal gland (200 pS) (Findlay, 1984). The open- and closed-time distributions reported here are also similar to those of the Ca^{2+}-activated K^+ channel (membrane potential 30 mV, $[Ca^{2+}]_{cytoplasm}$ 0.1 to 1 μM) in rat muscle investigated by Magleby and Pallotta (1983). However, the voltage dependence of the time-averaged open time is opposite to that found here, though it is interesting to note that this voltage dependence can be reversed at high cytoplasmic Ca^{2+} concentrations (Marty, Tan & Trautmann, 1984).

Therefore, a detailed understanding of these

K^+-selective channels (believed to be tonoplast channels), derived from a convenient system like cytoplasmic drops, is relevant to K^+ channels in the plasmalemmas of many Charophyte species as well as Ca^{2+}-activated K^+ channels which are ubiquitous in mammalian cells.

Conclusions

The unitary *I/V* relation is characteristic of diffusion-limited ion translocation through the K^+ channels. Läuger's theory (1976) of diffusion-limited ion flow is in good agreement with the data. We conclude that the diffusion of ions outside the pore is a major factor contributing to the channel conductance. The environment near the mouth of the pore is substantially different when the channel is open from that in the bulk solution phases. These effects must be considered when deriving intrinsic channel properties from the unitary *I/V* data.

The analysis of the channel open- and closed-time distributions indicates a minimum kinetic scheme that has three closed states, one open state and two reaction pathways connected to the open state. The proposed model which describes the voltage dependence of the open- and closed-time distributions is an eight-state model with one open state and seven closed states. The open- and closed-time data entirely accounts for the mean *I/V* characteristics indicating that long-lived dormant states are not significant to the steady-state macroscopic K^+ current. The mean *I/V* data for patches containing single and multiple channels show that cooperative effects within the K^+ channel population have little bearing on the macroscopic K^+ current.

We wish to thank Dr. Mary Beilby for many helpful discussions and for critically reading this manuscript. We acknowledge support from the ARGS and from the University of Sydney. The work was also supported by a National Research Fellowship.

References

Barrett, J.N., Magleby, K.L., Pallotta, B.S. 1982. Properties of single calcium-activated potassium channels in cultured rat muscle. *J. Physiol. (London)* **331**:211–230

Beilby, M.J. 1985. Potassium channels at *Chara* plasmalemma. *J. Exp. Bot.* **36**:228–239

Beilby, M.J. 1986. Factors controlling the K^+ conductance in *Chara*. *J. Membrane Biol.* **93**:187–193

Blatz, A.L., Magleby, K.L. 1986. Correcting single channel data for missed events. *Biophys. J.* **49**:967–980

Coleman, H.A., Findlay, G.P. 1985. Ion channels in the membrane of *Chara inflata*. *J. Membrane Biol.* **83**:109–118

Colquhoun, D., Hawkes, A.G. 1981. On the stochastic properties of single ion channels. *Proc. R. Soc. London B* **211**:205–235

Colquhoun, D., Hawkes, A.G. 1982. On the stochastic properties of bursts of single ion channel openings and of clusters of bursts. *Philos. Trans. R. Soc. London B* **300**:1–59

Colquhoun, D., Hawkes, A.G. 1983. The principles of the stochastic interpretation of ion-channel mechanisms. *In:* Single-channel recording. B. Sakmann and E. Neher, editors. pp. 135–175. Plenum, New York

Findlay, G.P., Hope, A.B. 1964. Ionic relations of cells of *Chara australis*. *Aust. J. Biol. Sci.* **17**:62–77

Findlay, I. 1984. A patch-clamp study of potassium channels and whole-cell currents in acinar cells of the mouse lacrimal gland. *J. Physiol. (London)* **350**:179–195

Hamill, O.P., Marty, A., Neher, E., Sakmann, B., Sigworth, F.J. 1981. Improved patch-clamp techniques for high-resolution current recording from cells and cell-free membrane patches. *Pfluegers Arch.* **391**:85–100

Inoue, I., Ishida, N., Kobatake, Y. 1973. Studies of excitable membrane formed on the surface of protoplasmic drops isolated from *Nitella*. IV. Excitability of the drop membrane in various compositions of the external salt solution. *Biochim. Biophys. Acta* **330**:27–38

Kamiya, N., Kuroda, K. 1957. Cell operation in *Nitella*. I. Cell amputation and effusion of the endoplasm. *Proc. Jpn. Acad.* **33**:149–152

Kolb, H.A., Köhler, K., Martinoia, E. 1987. Single potassium channels in membranes of isolated mesophyll *Barley* vacuoles. *J. Membrane Biol.* **95**:163–169

Läuger, P. 1976. Diffusion-limited ion flow through pores. *Biochim. Biophys. Acta* **455**:493–509

Lühring, H. 1986. Recording of single K^+ channels in the membrane of cytoplasmic drop of *Chara australis*. *Protoplasma* **133**:19–27

Magleby, K.L., Pallotta, B.S. 1983. Calcium dependence of open and shut interval distributions from calcium-activated potassium channels in cultured rat muscle. *J. Physiol. (London)* **344**:585–604

Marty, A., Tan, Y.P., Trautmann, A. 1984. Three types of calcium-dependent channels in rat lacrimal glands. *J. Physiol. (London)* **357**:293–325

Ohkawa, T., Tsutsui, I., Kishimoto, U. 1986. K^+ channel in the *Chara* plasmalemma: Estimations of K^+ channel density and single K^+ channel conductance. *Plant Cell Physiol.* **27**:1429–1438

Reeves, M., Shimmen, T., Tazawa, M. 1985. Ionic activity gradients across the surface membrane of cytoplasmic droplets prepared from *Chara australis*. *Plant Cell Physiol.* **26**:1185–1193

Sachs, F. 1983. Automated analysis of single-channel records. *In:* Single-Channel Recording. B. Sakmann and E. Neher, editors. pp. 265–284. Plenum, New York

Sakano, K., Tazawa, M. 1986. Tonoplast origin of the membrane of cytoplasmic droplets prepared from *Chara* internodal cells. *Protoplasma* **131**:247–249

Smith, F.A., Walker, N.A. 1978. Entry of methylammonium and ammonium ions into *Chara* internodal cells. *J. Exp. Bot.* **29**:107–120

Spanswick, R.M. 1970. Electrophysiological techniques and the magnitudes of the membrane potentials and resistances of *Nitella translucens*. *J. Exp. Bot.* **21**:617–627

Spanswick, R.M., Williams, E.J. 1964. Ca fluxes and membrane potentials in *Nitella translucens*. *J. Exp. Bot.* **16**:463–473

Svintitskikh, V.A., Andrianov, V.K., Bulychev, A.A. 1985. Photo-induced H^+ transport between chloroplasts and the cytoplasm in protoplasmic droplet of *Characeae*. *J. Exp. Bot.* **36**:1414–1429

Walker, N.A. 1980. The transport systems of charophyte giant algae and their integration into modes of behaviour. *In:* Plant Membrane Transport: Current Conceptual Issues. R.M. Spanswick, W.J. Lucas and J. Dainty, editors. pp. 287–304. Elsevier, Amsterdam

Received 2 April 1987; revised 19 August 1987